Injectable biodegradable chitosan-alginate hydrogel for gene delivery

Jingxuan Yan

A thesis

submitted in partial fulfillment of the

requirements for the degree of

Master of Science

University of Washington

2017

Committee:

James D. Bryers

Fumio S. Ohuchi

Program Authorized to Offer Degree:

Materials Science and Engineering

University of Washington

Abstract

Injectable biodegradable chitosan-alginate hydrogel for gene delivery

Jingxuan Yan

Chair of the Supervisory Committee:

Professor James D. Bryers

Department of Bioengineering

Currently, non-viral gene delivery vectors are widely used to encapsulate plasmid DNA or mRNA into nanoparticles that transport the genetic material to cells of interest. Although non-viral vectors have not received significant attention in the past because of their poor efficiency versus viral vectors, they have been proven bio-safe and not to elicit a severe immune response. The primary objective of this study was to develop and evaluate an injectable biodegradable chitosan-alginate hydrogel that will locally deliver a cationic polymer packaged plasmid DNA vector.

An evenly crosslinked hydrogel was prepared by mixing an oxidized alginate solution and a N-succinyl chitosan solution within a syringe at a volume ratio of 1:2. Hydrogels were characterized for gelation time, morphologies, mechanical properties, *in-vitro* swelling and degradation behaviors, protein adsorption, and cell toxicity. Nanoparticle "polyplexes" were formed by mixing anionic pDNA (pMAX-GFP) with cationic poly(ethylenimine) (**PEI**) in a Nitrogen/Phosphorous

(**N/P**) ratio =7. The resultant polyplexes were encapsulated into alginate-chitosan hydrogels and their *in-vitro* release kinetics were quantified. The *in-vitro* transfection of fibroblast (BHK) and dendritic cells (DC 2.4 and JAWsII cells) was quantified by transfected cell GFP gene expression at 1 day, 3 days and 5 days.

The chitosan-alginate hydrogels could be injected through state the size of the needle after gelling for around 2 minutes. The hydrogels were proven elastic materials with a compressive modulus between 1.08 to 3.58 kPa, which approximates soft tissues. The hydrophilic nature and high swelling ratios of the hydrogels (from 25.7 to 39.6) directly reflected their high efficiency of substance exchange. *In vitro*, the hydrogels were found degradable by hydrolysis with the degradation rate varying based on the chitosan-alginate composition. The *in-vitro* release test demonstrated that between 40-75% of pDNA/PEI polyplexes were continuously released from 10CS/50Alg hydrogel over 14 days mainly by diffusion. Cells (Baby hamster kidney (**BHK**) cells and two dendritic cell lines) both exhibited GFP gene transfection by day 5 while retaining high cell viability. As expected, the transfection efficiency of BHK cells was about ten times higher than that of either dendritic cell line.

Table of contents

Acknowledgements

I sincerely wish to express my deepest gratitude to my thesis advisor, Dr. James Bryers, for his support and dedicated mentorship on my research. I would like to thank my supervisory committee member, Dr. Fumio Ohuchi, for his knowledge and suggestions. I am deeply indebted the entire Bryers Lab, especially Dr. Ruying Chen and Dr. Hong Zhang, for their continuous suggestions, valuable conversations and troubleshooting. In addition, I am grateful to Robyn Francisco, Dr. Buddy Ratner, Tomas Hady, Alissa Bleem, Dr. Neal Beeman, Dr. Billianna Hwang, Zak Wescoe and Ian Dryg, for their help on my related researches. I would like to thank my family and my friends for their love and encouragement in my graduate study.

List of Abbreviations

BSA	Bovine serum albumin
CD	Cyclodextrin
DC	dendritic cell
DLS	dynamic light scattering
FBS	fetal bovine serum
GFP	green fluorescence protein
MHC	major histocompatibility complex
mRNA	messenger RNA
O-Alg	oxidized alginate
paCD	polycationic amphiphilic CD
PBAE	poly-β-amino esters
pDNA	plasmid DNA
PEI	poly(ethylenimine)
pHEMA	poly(hydroxyethylmethacrylate)
PLL	poly(L-lysine)
PMA	polymethacrylate
S-CS	N-succinyl chitosan
SEM	scanning electron microscopy

Chapter 1 Specific Aims

Gene-based nucleic acid vaccines are capable of eliciting protective immunity in humans to persistent pathogens, -*e.g.,* HIV, malaria, and tuberculosis, for which conventional protein/peptide vaccines have failed. Nucleic acid vaccines have the potential to address these needs, but despite decades of research there is still no commercial product for human use. Nucleic acid vaccines (pDNA, mRNA) have several advantages over protein antigen vaccines: *(a)* they lack the MHC haplotype restrictions of peptide/protein antigens and *(b)* nucleic acid vaccines are not subject to neutralization by the host immune response, thus allowing repeat boosting.

Recently, it has been proposed that *in vivo* modulation of host cell populations can be achieved using three-dimensional (3D) biomaterials with spatiotemporal control of biochemical and mechanical cues. However, 3D biomaterials are typically fabricated *in vitro*, requiring surgical placement in the body, and their preformed structures could limit the capability of host cells to organize themselves.

Here we propose an approach in which host immune cells could be recruited and modulated *in vivo* by 3D scaffolds that spontaneously assemble *in vivo* upon injection. This proposal seeks to maximize pDNA delivery and transfection by (a) cationic polymer packaging system to condense and neutralize anionc pDNA into nanoparticles (polyplexes) that would be released from an injectable self-gelling hydrogel delivery system.

Specific Aim 1. Hydrogel preparation and characterization

Specific Aim 2. *In-vitro* evaluation of pDNA/PEI polyplex delivery and transfection efficiency

Chapter 2 Hydrogels for gene delivery: potential and challenges

1. Introduction

By introducing foreign DNA or RNA into host cells, gene delivery has been widely used for the genetic modification of cells that offers a great potential to improve tissue regeneration and even treat active diseases.[1] Genes can be delivered into cells by two methods; modified viruses or non-viral vectors. Being achieved by DNA transduction process, virus mediated gene delivery is effective because the structure of the virus shields the DNA by from systemic degradation. However, viral gene delivery presents risks of genetic mutation and severe immune response. Alternatively, non-viral gene delivery utilizes anionically charged plasmid DNA or RNA.[2] But naked DNA or RNA molecules cannot enter cells efficiently because of their negatively charged phosphate groups and are susceptible to rapid degradation mediated by nucleases. Therefore, many non-viral vehicles have been designed and developed to encapsulate or condense plasmid DNA or RNA to form nanoparticles that transport the target nucleic acids into cells.[3] Compared to modified viruses, non-viral gene delivery has several advantages, such as: repeated applications due to a relatively high bio-safety profile. In addition, larger genes can be delivered by non-viral gene delivery vectors versus viruses. However, the primary bottleneck of non-viral vectors is their low transfection efficiency.[4]

2. Obstacles to non-viral gene delivery

DNA complexes (nanoparticles) are formed through condensing or shielding by non-viral vectors; then enter the cell by endocytosis (**Figure 2.1**). Different cells utilize various endocytosis pathways: clathrin-dependent endocytic pathways, caveolae, macropinocytosis and phagocytosis. For example, immature dendritic cells (DC) engulf extracellular solute by macropinocytosis. Macropinocytosis is a clathrin-independent process that involves cell membrane ruffling and folding back onto itself to form macropinosomes (**Figure 2.2**).[5] Early endosomes are the first components of endocytosis that are located in the periphery of cell. Part of the nucleic acids are released from late endosomes, which is called "endosomal escape", while others are degraded by lysosomes. The commonly used cationic polymers as non-viral vehicles have abundance of amino groups that further provides a "proton sponge" effect which facilitate the release of nucleic acid in cytoplasm. Briefly, the continuous influx of protons (H^+) and passive entry of chloride ions (Cl^-) by the amino groups within endosomes leads to the rupture of endosomal membrane (**Figure 2.3**).[6] Messenger RNA (mRNA) migrates to ribosome and starts translation directly, while plasmid DNA (pDNA) has to be translocated into nucleus first before gene transcription.

Another major obstacle to non-viral gene delivery is the disassembly of nucleic acid complexes after their endosomal escape. It still remains unsure that whether the escaped staffs are naked nucleic acids or nucleic acid-polymer complexes, but it is proven that the strong DNA binding with high-molecular-weight cationic polymers inhibits transfection although it facilitates cellular uptake. Therefore, an optimization of N/P ratio is necessary to maximize the transfection efficiency.

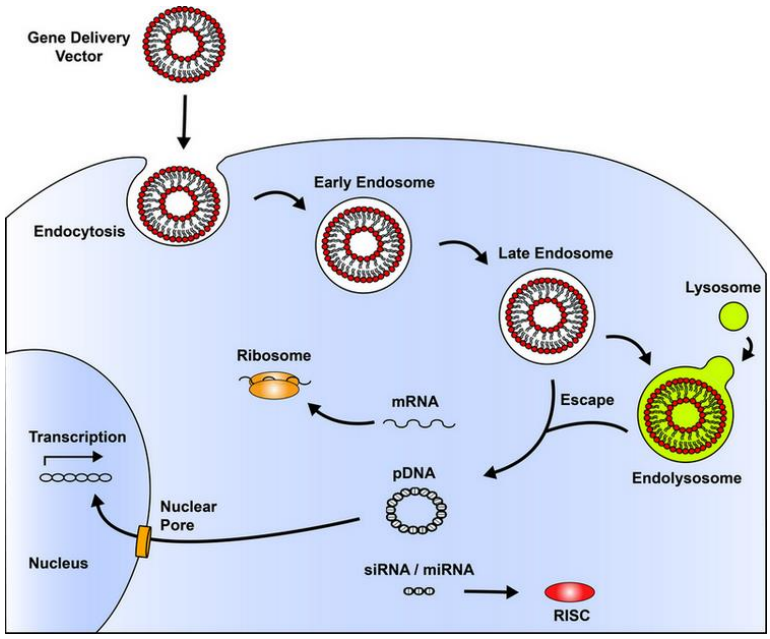

Figure 2.1 Extracellular and intracellular barriers to gene delivery and expression.

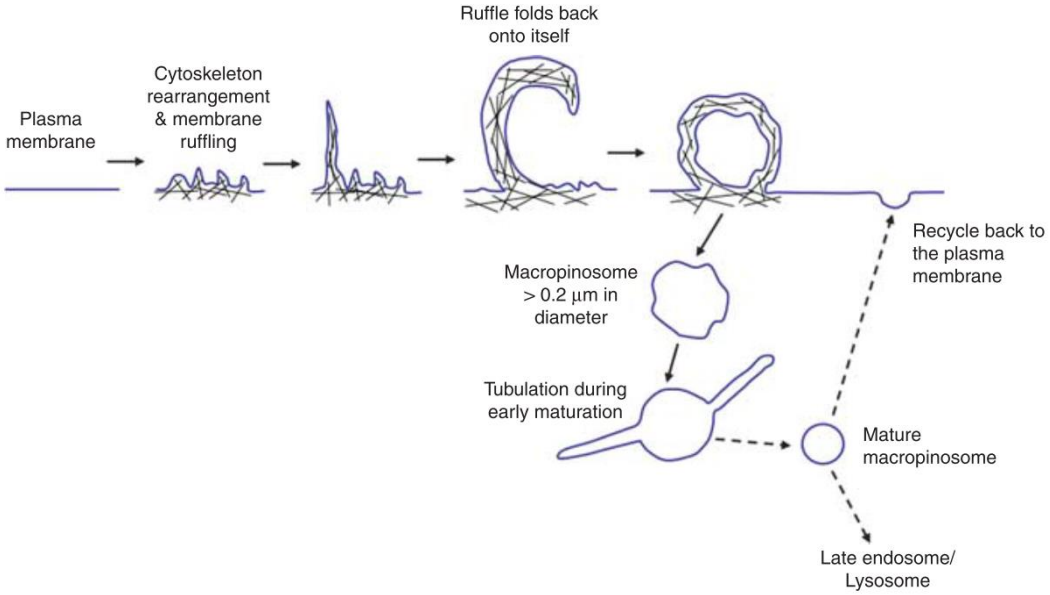

Figure 2.2 Pathway of macropinocytosis.

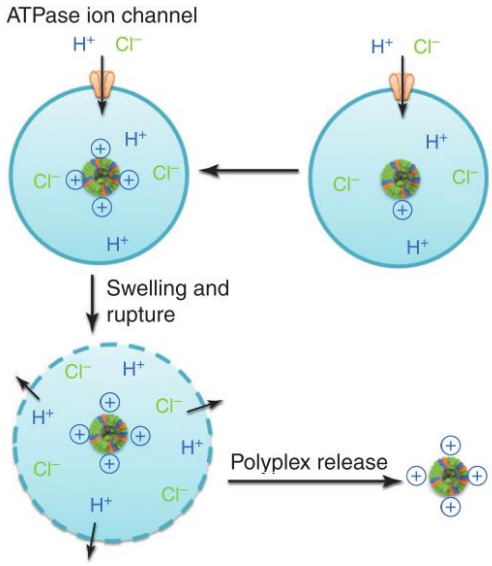

Figure 2.3 Endosomal escape of nucleic acid polyplexes through the "proton sponge" effect.

3. Non-viral gene delivery

Being considered as a safe and efficient therapeutic strategy to promote tissue regeneration and treat cancer or other diseases, non-viral gene delivery has been developed for decades to improve the transfection efficiency by different vectors including cationic polymers and liposomes.[4][7]

3.1. Cationic polymers

Cationic polymers can easily form polyelectrolyte complexes (polyplexes) with anionic plasmid DNA or RNA via condensing nucleic acids into particles, thus protecting them from enzymatic degradation. Typically, the slightly positive charges on DNA or RNA polyplexes facilitate cell uptake because of the electrostatic attraction between polyplexes and cells.[8] Recently investigated cationic polymers include poly(ethylenimine), poly (L-lysine), poly-β-amino esters, branched polyaminoesters, polymethacrylate, cyclodextrin, chitosan, dendrimers, polysaccharide-based polymers and polydisulfide amines, and miscellaneous polyamines.

PEI has been widely reported as an excellent non-viral vector for gene delivery system.[3] Typically, linear PEI has numerous positive charges because of the repeating amine groups on the backbone. Compared with other commercially available transfection vectors, PEI is stable with high transfection ability that helped it to gain increasing attention in the past decade and more derivatives have been developed as gene carriers.[4][9] An optimal transfection performance usually requires excessive linear PEI to decrease the size of DNA or RNA polyplexes for cellular uptake.[10] However, a large amount of PEI polymers is toxic to cells because of cellular membrane damage, which gives PEI into an efficiency-cytotoxicity dilemma.[11]

Poly (L-lysine) (PLL) is a class of linear polypeptides (L-lysine) with high positive charge density that allows them to condense negatively charged nucleic acids. Although histidine residues were

used to graft onto the backbone of PLL to enhance endosome escape, the relatively low transfection efficiency blocks its application on non-viral gene delivery.[12]

Chitosan is a linear polysaccharide with high positive charges and another research hotspot in non-viral gene delivery system.[13] It has been proven highly biocompatible and osteoconductive, but the transfection efficiency is affected by its molecular weight and degree of deacetylation.[14] DNA polyplexes formed by low-molecular-weight chitosan have a high stability, but the particle size increases with the increasing chitosan polymer chain. The limitation of using chitosan as a non-viral vector is its low solubility and inefficient gene uptake.[15] Cyclodextrin (CD) is a type of naturally derived cyclic (α-1,4)-linked oligosaccharide of α-D-glucopyranose. Native CDs cannot form stable complexes with pDNA, which limits their application on gene delivery. However, in recent decades, numerous CD derivatives have been developed to improve transfection efficiency, such as polycationic amphiphilic CDs (paCDs). [16]

Poly-β-amino esters (PBAE) has been recently developed for gene delivery vectors. The degradable PBAE shows high gene transfection efficiency and low cytotoxicity simultaneously at high molecular weight and high branched structure.[17] Polymethacrylate (PMA) has been emerging as an alternative non-viral vectors for gene delivery recently. PMA copolymers with functionalities were synthesized and their physicochemical and biological properties including cellular uptake and endosomal escape were investigated. [18] Polyamines is another degradable cationic vehicle for non-viral gene delivery. A study has demonstrated that the low-molecular-weight polyamines could transfect brain capillary endothelial cells with negligible cytotoxicity.[19]

Dendrimers consist of a core molecule and a number of highly branched molecules as arms. Compared to other cationic polymers, dendrimers have a well defined size and structure due to the

specific stepwise method of synthesis. As a result, the high density of terminal groups help minimize the cytotoxicity and offer multiple attachment sites for targeting moieties.[20]

3.2. Liposomes

Cationic lipid-based polymers have been proven quite effective for DNA and RNA delivery by endocytosis.[13][21] All of them share the common structure of hydrophilic head and hydrophobic tail. The hydrophilic heads, usually positively charged, bind with negatively charged nucleic acids by electrostatic forces. The hydrophobic tails link together and form liposome structures.[1] Lipid-based polymers have shown biocompatibility and high transfection efficiency due to their positive charges that interact with negatively charged cell membranes as well as their liposome structure that improves cellular uptake.[22] Similar to PEI, liposomes can become cytotoxic if the ratio of lipid to DNA exceeds 3. Further, the poor stability and rapid clearance of cationic lipids limits their application on gene delivery because the initial goal of using non-viral vector is to improve the circulation half-life of nucleic acids. The liposome transfection efficiency depends on the nature of head and tail functional groups, the fraction of charged groups, and the liposome particle size.[23] In addition, the negatively charged proteins and enzymes *in vivo* may also interact with liposomes, and result in weak cell adhesion and low transfection.[13]

4. Injectable hydrogels

Recent literature has shown that the gene expression seen from vectors delivered from implantable 3D porous polymer scaffolds trigger far better transfection efficiency than repeated systemic injections.[24][25] Hydrogels are one class of such polymers seeing application in tissue engineering, sustained-release drug delivery, and gene delivery due to their unique properties.[26][27][28][29][30] A hydrogel is basically a crosslinked network of polymers that are absorbent, hydrophilic and elastic, with a similar physical profile to soft tissues. Hydrogels made by naturally derived polymers (like polysaccharides and proteins) and synthetic polymers - like poly(hydroxyethylmethacrylate) (pHEMA) and poly(ethylene glycol) (PEG) both exhibit biocompatibility *in vitro* and *in vivo*.[31] Numerous methods have been developed for hydrogel preparation including physical and chemical crosslinking.

4.1. Hydrogels by physical crosslinking

Ionic crosslinking is one of the most widely used methods to crosslink polymer chains. Basically, metal cations such as Ca^{2+} and Fe^{3+} can bind with negatively charged groups, like ($-COO^-$), in the polymer. For example, the sodium ion can be replaced by calcium cations rapidly when introducing $CaCl_2$ into Na-alginate solution.[32] Although the stronger binding of calcium cations with carboxyl groups in alginate offers a convenient way to develop a hydrogel, the fast and uncontrollable reaction rate prompted researchers to optimize the process. Alginate hydrogels fabricated by ionic crosslinking have been investigated for tissue engineering application for years; one of the major drawbacks to alginate gels is their fast degradation rate both *in vitro* and *in vivo*. The crosslinker, calcium cations, can be displaced with other metal cations due to the swelling behavior of hydrogel under physiologic condition. Another problem is toxicity to the surrounding tissues that caused by excess calcium cations released from alginate during its degradation.[33]

4.2. Hydrogels by chemical crosslinking

Comparing with physical/ionic crosslinking, chemical crosslinking hydrogels usually exhibits stable and homogeneous networks due to the strong covalent bonding.

Disulfide bonds are formed between two thiol groups that play an important role in protein folding. Basically, an oxidative agent, such as hydrogen peroxide, is required to crosslink two polymers via disulfide bonds. Hydrogels formed by disulfide crosslinking have a suitable and controllable gelation time of ~5 minutes, but one of the major issues is in protein delivery.[34] The thiol group of cysteine in the protein can form bonds with the thiol groups in the hydrogels that negatively influences degree of crosslinking and properties of the final hydrogel.

Michael-type addition reaction commonly refers to the 1,4 addition of nucleophile-like thiols or amines added to unsaturated carbonyl compounds.[35] Michael-addition crosslinking with amine groups needs elevated temperatures and an alkaline environment, which are not possible when preparing hydrogels in physiological conditions. For *in situ* forming hydrogels, thiol groups are preferred for the addition reaction. Besides, the conjugation of thiol groups next to positively or negatively charged amino acids is able to control the gelation time from between 1 to 14 minutes thus allowing possible injection of a solution prior to gelling *in vivo*.[36] More importantly, hydrogels crosslinked by Michael-type addition reactions have proven biocompatible and biodegradable.

Enzymatic reactions are another widely used method of hydrogel formation. To form isopeptide bond between two polymers with amino groups and carboxyl groups, transglutaminase is added to drive the enzymatic reaction under physiological conditions.[37] Enzymatic crosslinked hydrogels can be prepared by either proteins or grafting peptides onto polymer backbones with both options showing great biocompatibility.[38] In addition, the isopeptide bonds between two polymers varies

with enzyme concentration, but are strong enough to make the hydrogel stable under *in vivo* conditions.

By self-assembly crosslinking and thermo-responsive phase change, certain hydrogels can form *in situ* upon injection. But these two methods have the same liability- weak bonds between polymers. The weak interacting force involved in crosslinking of these two methods (*e.g.,* electrostatic attraction, hydrogen binding, cohesive interactions by phase transition) do not form stable networks within hydrogels. Their low storage modulus is another critical bottleneck for their application in biomedical engineering.[31]

Schiff-base reactions, another covalent crosslinking method, forms carbon-nitrogen double bonds ($-\mathrm{C}=\mathrm{N}-$) upon mixing two polymers with amino groups and aldehyde groups, respectively. The strength of crosslinking depends on the fraction of functional groups. The rapid and reversible Schiff-base reaction provides the hydrogel with both stable structure and biodegradable properties. More importantly, numerous naturally-derived polymers can be used to prepare injectable and biodegradable hydrogels by Schiff-base reaction.[27] For example, the active amino groups on chitosan and proteins make them ideal candidates for hydrogel formation.[39] In addition, by employing oxidization of polysaccharides, like alginate and hyaluronic acid, aldehyde groups are introduced on their backbones.[40] Although synthetic polymers have tunable mechanical properties and degradation profiles, naturally-derived polymers usually have better interaction with cells.

In this present study, an injectable biodegradable chitosan-alginate hydrogel is developed for sustained-release of pDNA/PEI polyplexes. For hydrogel preparation, succinic anhydride was grafted onto chitosan to improve its solubility and alginate was oxidized by sodium periodate to obtain aldehyde groups on its polymer chain. Hydrogels were systematically characterized first,

then the polyplexes release behavior as well as transfection of fibroblast and dendritic cells were both analyzed *in vitro*.

Chapter 3 Hydrogel preparation and characterization

1. Experimental methods

1.1. Materials

Chitosan (50,000-190,000 Da, 75-85% deacetylated), lactic acid (~90%), methanol, succinic anhydride (≥99%) and sodium periodate (≥99.8%) were supplied by Sigma-Aldrich. Sodium alginate was purchased from Spectrum Chemical Manufacturing Corporation. Ethylene glycol (≥99%) was supplied by J.T. Baker Chemicals (Avantor Performance Materials). Bovine serum albumin (BSA) was purchased from Thermo Fisher Scientific Inc. (USA). All chemicals were used as received.

1.2. Synthesis of N-succinyl chitosan

Chitosan (1 g) was dissolved in 80 mL lactic acid (5% v/v). The chitosan solution was then diluted by 320 mL methanol with magnetic stirring. Succinic anhydride (2 g) was added gently into the solution and stirred at 600 rpm for 24 hours at room temperature. White floccules were produced in the solution after increasing the pH value to about 8.0 by adding NaOH solution (0.1 M). The produced N-succinyl chitosan was centrifuged at 2500 rpm for 5 min and dissolved by ultrapure water. The solution was further purified by dialysis against ultrapure water for 3 days. The purified solution was then lyophilized at -50 ºC to obtain solid N-succinyl chitosan (S-CS), which was collected and stored at room temperature.

1.3. Synthesis of oxidized alginate

Sodium alginate (3 g) was dissolved in 200 mL deionized water to obtain an alginate solution of 1.5% (w/v) concentration. Prepared sodium periodate solution (15% w/v, 10 mL) was added dropwise into the alginate solution. The oxidation reaction occurred thoroughly by magnetic stirring at 600 rpm for 24 hours at room temperature in dark. Ethylene glycol (2 mL) was added

and mixed for 2 hours to stop the oxidization reaction. The solid oxidized alginate (O-Alg) was finally purified by a 3-day dialysis against ultrapure water and lyophilization at -50 ºC. The oxidized alginate was collected and stored at room temperature.

1.4. Preparation of hydrogels

S-CS and O-Alg were dissolved in PBS separately before hydrogel formation. Four hydrogels with different compositions were prepared and investigated according to Table 1. To form an evenly crosslinked hydrogel, O-Alg solution and S-CS solution were mixed thoroughly in the injector at a volume ratio of 1:2. The hydrogels were either injected out onto a dish or formed within a columned shape for further test and investigation. The sol-gel transition was monitored at room temperature and the gelation time was tested by inclining tube.

Table 1. Concentration of S-CS and O-Alg for hydrogel preparation.

Hydrogel samples	S-CS (% w/v)	O-Alg (% w/v)	O-Alg/S-CS (v/v)
15CS/50Alg	15	50	1:2
10CS/50Alg	10	50	1:2
15CS/100Alg	15	100	1:2
10CS/100Alg	10	100	1:2

1.5. Mechanical tests

The columned hydrogel samples (12 mm diameter, 10 mm height) were prepared in a syringe as previously described. Mechanical properties of hydrogels were characterized by compressive test in unconfined conditions. The compressive stress-strain curves of hydrogels were determined by a mechanical analyzer (Instron) at a deformation rate of 1 mm/min at room temperature after gelling for 10 min. Compressive moduli were calculated from the linear region of stress-strain curves.

1.6. Swelling and in-vitro degradation

To characterize the swelling behavior of hydrogels, columned samples were immersed in PBS (pH=7.4) at 37 ºC for 2 hours. The swollen hydrogels were taken out of tubes and the wet-state weight (W_s) was immediately recorded after the excess PBS on the hydrogel surface were eliminated by filter paper. The dry-state weight (W_d) of hydrogel was measured after being lyophilized at -50 ºC for 48 hours. The swelling ratio (SR) was determined as $(W_s - W_d)/W_d$.

The kinetics of weight loss of hydrogels in PBS and PBS-BSA (20% w/v) medium was monitored over 2 weeks. The initial weight of hydrogels (W_0) were measured immediately after hydrogel formation. Samples were immersed into 30 mL PBS or PBS-BSA (20% w/v) medium then placed into an incubator with a shaking table at 70 rpm and a constant temperature at 37 ºC. Hydrogels were weighted (W_t) after removing the residual medium on the surface of samples at the various time points of measurement. Medium was replaced every day. The hydrogel remaining mass was defined as $W_t/W_0 \times 100\%$.

1.7. Protein adsorption

Hydrogel samples were prepared in a syringe and incubated in 50 mL tubes with 20 mL PBS-BSA (20% w/v) medium for 24 hours at 37 ºC after weighting (*M*). The initial concentration of BSA (C_0) in the medium and that after 24-hour incubation (C_1) were measured by the BCA™ assay carried out in a Nanodrop instrument. The medium was then replaced by PBS of the same volume and samples were incubated at 37 ºC for another 24 hours before measuring the BSA concentration (C_2) in PBS. Protein adsorption was defined as $(C_0V - C_1V)/M$ and the released protein after 24-hour incubation in PBS was calculated by C_2V/M, where *V* equals to 20 mL. The protein blocked within the hydrogel was the difference between protein adsorption in the first 24 hours and the protein release in the second 24 hours.

1.8. Cell viability

All cell culture media and reagents were obtained from Gibco. BHK-21 hamster fibroblast cell line (ATCC) was maintained in Eagle's Medium supplemented with 10% FBS and 1% penicillin-streptomycin. The DC2.4 murine dendritic cell line (a gift from K.L. Rock, University of Massachusetts Medical School) was maintained in RPMI 1640 medium containing L-glutamine supplemented with 10 mM HEPES, 0.1 mM non-essential amino acids, 55 μM 2-mercaptoethanol, 10% FBS, and 1% penicillin-streptomycin. The JAWsII murine dendritic cell line (ATCC) was maintained in alpha minimum essential medium supplemented with 1.5g/L sodium bicarbonate, 2 mM L-glutamine, 5ng/mL GM-CSF, 20% FBS, and 1% penicillin-streptomycin.

Cells were seeded on the bottom of treated 24-well tissue culture plates at a concentration of 150,000 cells/well. The cells were cultured at 37 ºC for 4 hours to let them adhere. Culture medium was removed and 50 μL hydrogel samples were injected into the wells. 1 mL culture medium was added, and cells were incubated at 37 ºC. After 1-day, 3-day and 5-day culture, 100 μL of cell culture medium was first added into each well and an additional 100 μL of LIVE/DEAD stain (Invitrogen L-3324) was added to each well after completely removing culture medium and washing by PBS. Cells were then incubated for 20 min at 37 ºC in dark and imaged by a Zeiss Axio Observer Z1 fluorescence microscope.

1.9. Morphological observation

The microscopic morphologies of hydrogels were characterized using a scanning electron microscope (FEI SEM XL Siron). The samples were imaged at 3 kV accelerating voltage with 5 mm working distance after being lyophilized at −50 °C for 2 days, sliced and gold-coated for 90s.

2. Results and discussion

2.1. Hydrogel formation

The hydrogels were prepared by crosslinking N-succinyl chitosan (S-CS) with oxidized alginate (O-Alg) upon mixing (**Figure 3.1 a**). By introducing hydrophilic groups (succinic anhydride) into chitosan backbones, the water solubility of chitosan was increased from 1 mg/mL to 20 mg/mL. Oxidization of alginate not only introduced aldehyde groups on its polymer chain but reduced the molecular weight by 50% approximately. As a result, an oxidized alginate with a high solubility (100 mg/mL) was produced. The crosslinking of hydrogel was achieved by C=N bonds of Schiff-base reaction by amino groups on S-CS and the aldehyde groups on O-Alg. The SEM images illustrate its porous structure with interconnected pores (**Figure 3.1 c**). The pore size of hydrogel ranged from 100 to 200 µm after being lyophilized. Schiff-base reaction exhibited a controlled sol-to-gel phase transition behavior that is beneficial for an evenly crosslinking hydrogel formation in the syringe. The *in-situ* forming homogeneous hydrogel could be easily injected through 27G needle after gelling for around 2 minutes (**Figure 3.1 b**).

Gelation time is one of the significant profiles of injectable hydrogels. On the one hand, hydrogels with a short gelation time usually have an inhomogeneous crosslinking and pose great difficulties in applications. On the other hand, hydrogels with a long period time of gelation limit their *in-situ* forming properties. The ideal optimal gelation time of injectable hydrogel is ~1-10 minutes.[31] The sol-to-gel transition process was observed by inclining tubes (**Figure 3.2 a**). The gelation time was also measured by this method. As a result, hydrogels were formed within several minutes after mixing S-CS and O-Alg solutions (**Figure 3.2 b**). The gelation time varied from 49.7 to 149.7 seconds depending on the chitosan-alginate composition. It was found that a high concentration of S-CS helped shorten gelation time because of its high viscosity and introduction of more amino

groups for crosslinking. Hydrogels formed with higher concentration of O-Alg exhibited longer gelation times.

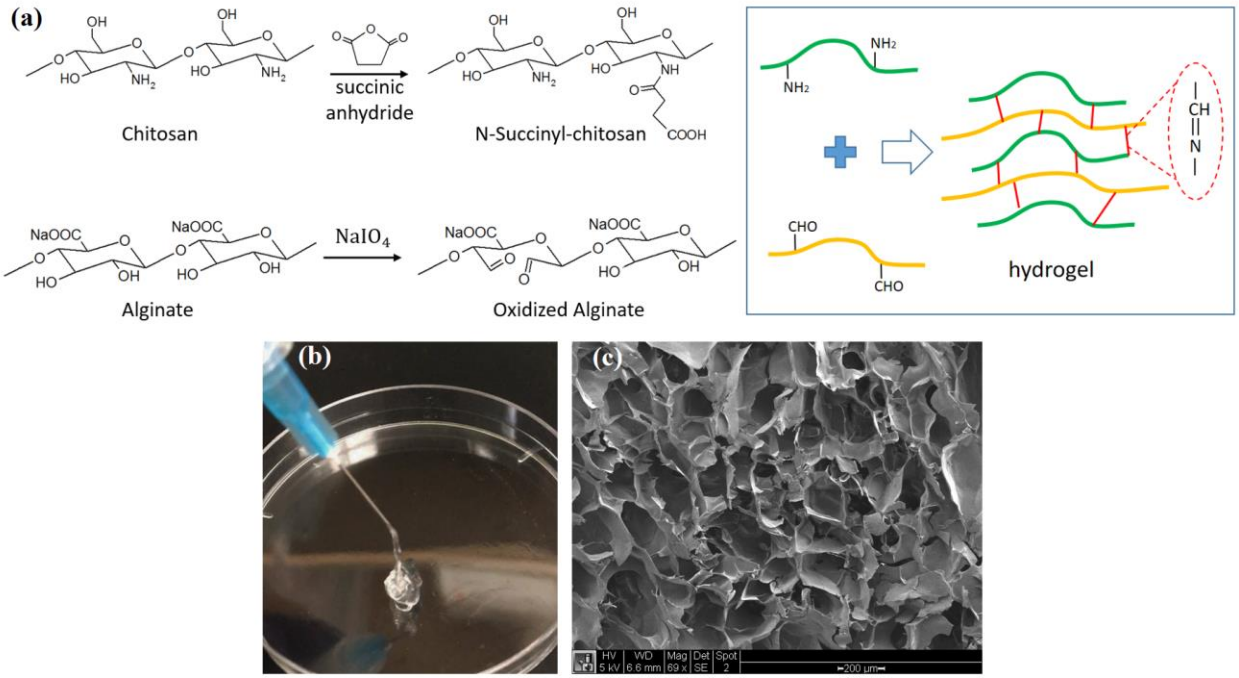

Figure 3.1 (a) Schematic illustration of chitosan-alginate hydrogel via Schiff-base reaction. Hydrogel injection (b) and the SEM image of the lyophilized 10CS/50Alg hydrogel sample.

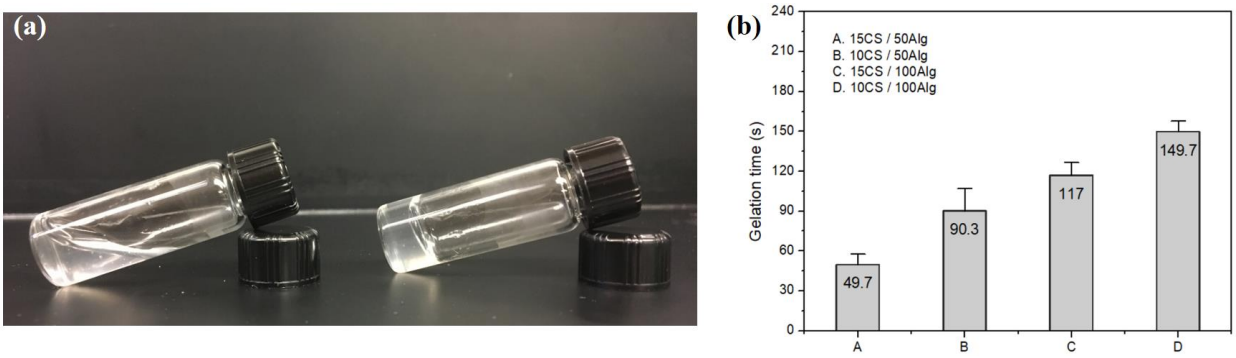

Figure 3.2 (a) Images to show sol (left) to gel (right) transition of hydrogel. (b) Gelation time of hydrogels were measured by inclining tube. Values reported are an average n=3, ±standard deviation.

2.2. Mechanical properties

As a local delivery system that is injected subcutaneously, hydrogels should exhibit similar mechanical properties comparable to soft tissues.[25] Mechanical properties of the hydrogels were

studied by an unconfined compressive test using a mechanical tester (**Figure 3.3 a**). The maximal strain varied from about 60% to 80%, which proved that hydrogels could be compressed by a large deformation without breaking to pieces. In addition, the linear relationship of compressive stress versus strain ranging from 0 to 15% demonstrated the elastic properties of hydrogels when they suffered from a small deformation (**Figure 3.3 b**). The compressive modulus was calculated in the linear range of the strain was 10% (**Figure 3.3 c**). The modulus was dependent on the degree of crosslinking to some extent. Typically, the hydrogel with a higher composition of S-CS and O-Alg (15CS/100Alg) had a higher compressive modulus (3.58 kPa) because of its stronger crosslinking network, while the weaker crosslinking within 10CS/50Alg hydrogel showed a lower modulus (1.08 kPa). However, all the hydrogels showed moduli similar with that of soft tissues (1-10 kPa), which indicated the appearance of a suitable biomaterial for applications in local delivery by subcutaneous injection.

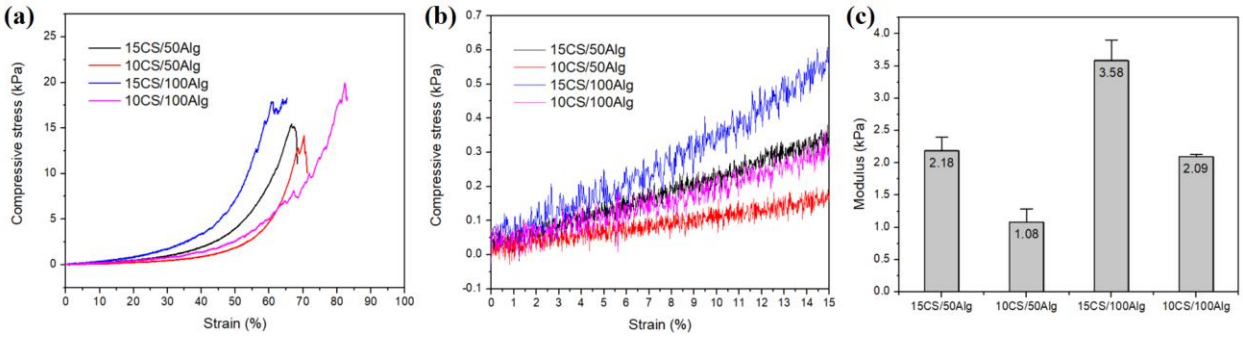

Figure 3.3 (a) Compressive stress-strain curve of hydrogels with different S-CS and O-Alg concentrations. (b) Enlarged image of stress-strain curve for strain ranging from 0 to 15%. (c) Compressive modulus of hydrogels calculated from the linear region of stress-strain curves. Values reported are an average n=3, ±standard deviation.

2.3. Swelling and degradation behavior

Swelling abilities of hydrogels are of great significance for substance exchange in tissue regeneration and drug release. The swelling ratio directly reflects the efficiency of substance absorption and excretion, which is one of the most important factors of release kinetics.[41] The

equilibrium swelling ratio of hydrogels with different S-CS and O-Alg composition were measured in PBS at 37 ºC over 2 hours (**Figure 3.4 a**). Results showed that all the hydrogels could absorb a large amount of water and their swelling abilities were depended on S-CS and O-Alg composition. The weight loss of hydrogels was monitored in PBS at 37 ºC as a function of time (**Figure 3.4 b**). In general, the 10CS/50Alg hydrogel was more readily degradable than the other hydrogels basically due to its weaker crosslinking which correlates with its lower compressive modulus. Also, its higher swelling ratio (39.6) could accelerate the degradation process. As a result, only 60.2% of 10CS/50Alg hydrogel remained at 10 days and samples broke into pieces at 14 days since the crosslinking of network was too weak to maintain its shape. For the other hydrogels with higher S-CS or O-Alg composition, their volumes decreased more slowly and about 70% mass remained after 2 weeks. To investigate the influence of protein on the degradation behavior of hydrogels, BSA was introduced into the PBS medium at a concentration of 20% w/v (**Figure 3.4 c**). It was found that the degradation rate of hydrogels was significantly increased by BSA in the medium. For example, the network of 10CS/50Alg hydrogel completely collapsed after 5 days in PBS-BSA medium while it lasted for 2 weeks in PBS without BSA.

The degradation behavior of hydrogel is mainly attributed to the reverse Schiff-base reaction and hydrolysis of both polysaccharides. The hydrogel absorbs water that promotes the cleavage of C=N bonds. The newly produced free chitosan and alginate polymers are hydrolyzed, and their molecular weights are decreased and the chemical structure are changed. The network becomes weaker so that hydrogels can absorb more water to shift the chemical equilibrium to left, which promotes degradation. This process continues until the network of hydrogel is too weak to maintain its shape.

The *in-vivo* degradation products of the hydrogel are another critical aspect that worthwhile to be discussed. It is commonly agreed that chitosan is hydrolyzed by lysozyme *in vivo* by breaking glucosamine-glucosamine bonds that result in chitosan oligosaccharides.[42] The oligosaccharides are then incorporated into glycoprotein pathways, metabolic pathways or excreted. [14][43] For alginate, it is known that the *in vivo* degradation of pure alginate is hard (> 6 months) and unpredictable due to lack of natural enzymes in human organisms.[44] Research has proved that oxidized alginate can be hydrolyzed within 2 months *in vivo* and is easily eliminated by kidneys.[41][45][46]

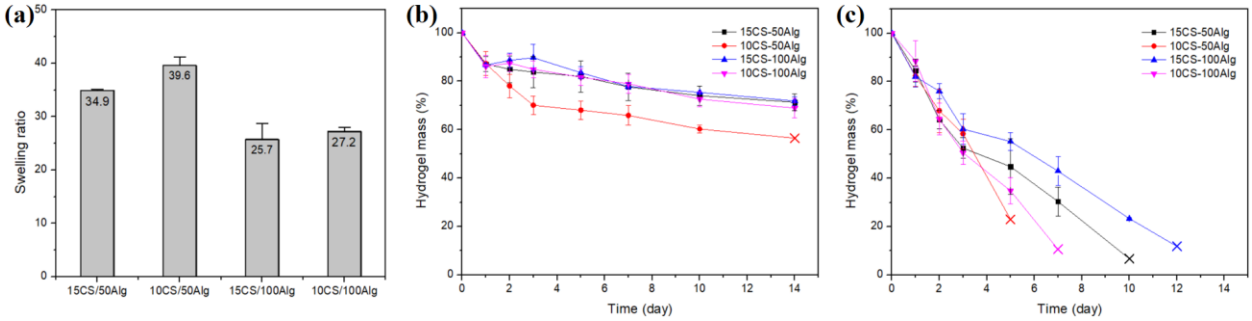

Figure 3.4 (a) Swelling ratio after two hours (a) and *in-vitro* degradation of hydrogels in PBS (b) and PBS-BSA (20% w/v) (c) at 37 ºC. Values reported are an average n=3, ±standard deviation.

2.4. Protein adsorption

Protein accumulation on the surface of biomaterials can be beneficial but can also cause problems. On the one hand, these proteins can promote the attachment of cells that facilitates drug uptake. On the other hand, protein adsorption is undesired in biomaterials field because it can invoke severe immune responses and lead to chronic inflammation.[44] The main factors of protein adsorption include surface energy, hydrophobicity, charges and intermolecular forces. The protein adsorption of hydrogels was measured as described previously, and the results were shown in **Figure 3.5**. Basically, all the hydrogels were proven hydrophilic due to the small values of protein adsorption. The higher protein adsorption of 10CS/50Alg hydrogel (30.5 mg/g) after 24-hour

incubation in PBS-BSA (20% w/v) is partially attributed to its relatively high swelling behavior. Proteins were not only adsorbed onto hydrogel surface but absorbed within the hydrogel.

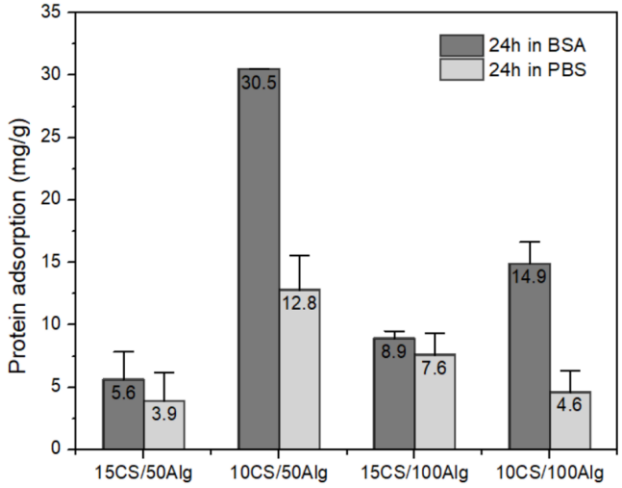

Figure 3.5 Protein adsorbed by hydrogels after 24 hours in PBS-BSA (20% w/v) (dark grey bars) then another 24 hours in PBS (light grey bars) at 37 ºC. Values reported are an average n=3, ±standard deviation.

2.5. Biocompatibility

Cell viability studies were performed to test the toxicity of hydrogels to mammalian cells. To test the cytocompatibility of hydrogel, a Live/Dead assay™ was used to stain both fibroblast and dendritic cells. The images were taken at 1 day, 3 days and 5 days, which were shown in **Figure 3.6 a-c**.

In general, chitosan/alginate hydrogel was proved very biocompatible to cells since there were no significant differences in cell viability compared to control groups without hydrogel. Majority of cells cultured with hydrogels were viable (green) and demonstrated no clear difference in viability between samples. When cultured with hydrogel, cells became larger and the number decreased. One plausible reason was that cells absorbed water from hydrogels. In addition, hydrogels degraded thoroughly after 5 days, which agreed with the result of the *in-vitro* degradation test. The pH value (**Figure 3.6 d-f**) suggested that the hydrogel degradation did lower pH. It was also found

that dendritic cells could survive and even proliferate in an acidic condition. It makes sense because the development of acidic environment is another hallmark of inflammatory processes.

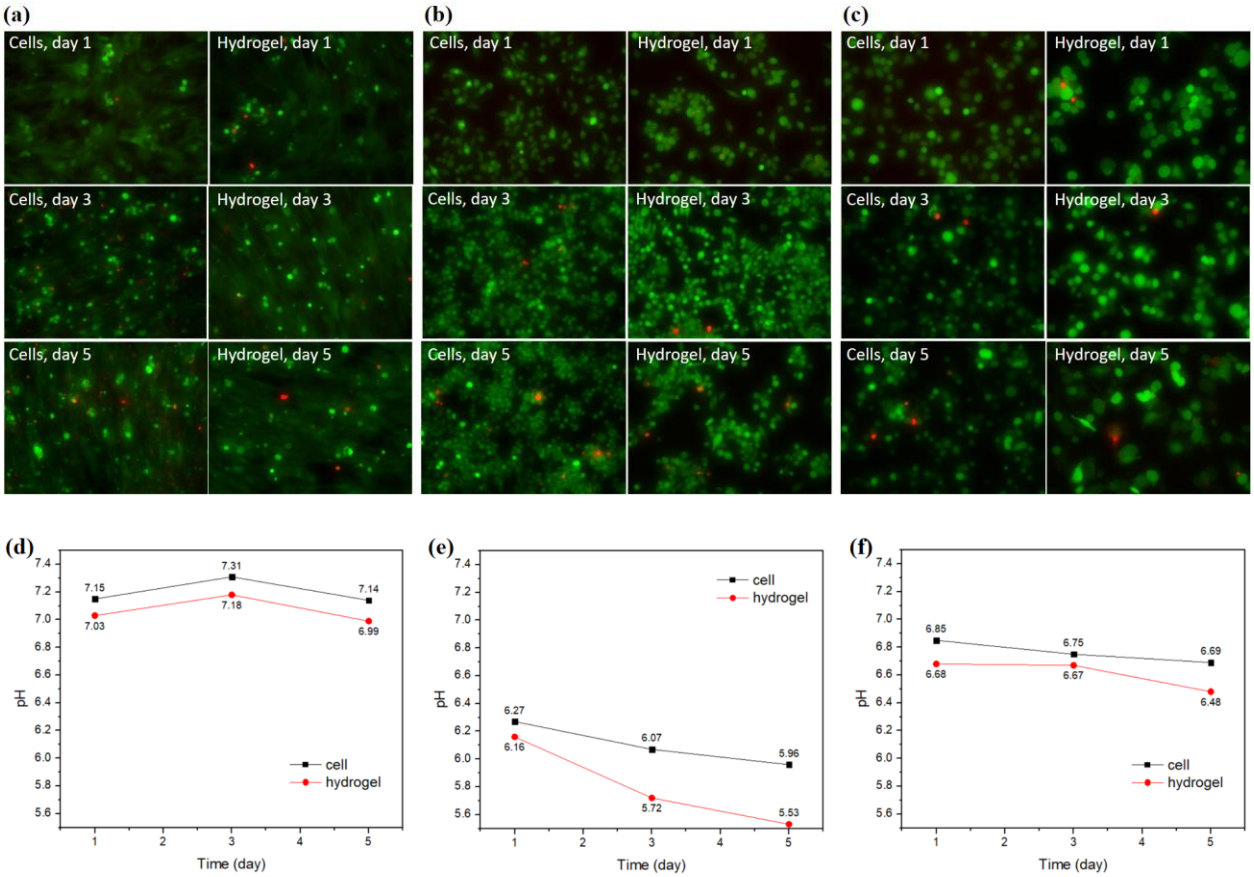

Figure 3.6 BHK (a), DC 2.4 (b) and JAWsII (c) cell viability by staining with Live/Dead assay. Cells were seeded at 150,000 #/well and 50 μL of 10CS/50Alg hydrogel was injected. Pictures of cells (left) and cells with hydrogel (right) were taken by inverted microscope (20×) at 1 day, 3 days and 5 days. pH value of BHK (d), DC 2.4 (e) and JAWsII (f) cell culture medium was also monitored at each time point.

3. Conclusions

Chitosan/alginate hydrogels were prepared, and their properties were systematically investigated, including gelation, mechanical properties, degradation behavior, protein adsorption and cytotoxicity. Hydrogels were formed in the syringe by mixing N-succinyl chitosan and oxidized alginate solution as a volume ratio of 2:1. The hydrogel was then able to be injected out through needle after gelling for around 2 minutes. Hydrogels were demonstrated to be elastic materials when suffered with a small deformation and the compressive modulus ranged from 1.08 to 3.58 kPa, which is close to that of soft tissues. These hydrogels were also hydrophilic materials that could absorb and contain a large amount of water. The *in-vitro* degradation test demonstrated that the hydrogels were degradable and proteins in the medium could accelerate the degradation process. Hydrogels could maintain their network structure for ~2 weeks in PBS, but they were found degraded within 5-12 days in PBS-BSA (20% w/v) solutions. These properties of hydrogel were related to the degree of crosslinking by the Schiff-base reaction. Basically, the hydrogel with a stronger crosslinking of network had a higher compressive modulus and lower swelling ratio. As a result, it took longer to be completely degraded *in vitro*. These hydrogels were demonstrated nontoxic and biocompatible by cell viability test despite making the culture medium mildly acidic. Provided these results, these chitosan-alginate hydrogels have significant potential as an injectable degradable biomaterial for local delivery.

Chapter 4 *In-vitro* evaluation of pDNA/PEI polyplex delivery and transfection efficiency

1. Experimental methods

1.1. pDNA/PEI polyplex formation

Plasmid pMAX-GFP (a gift from Dr. S. Pun, Department of Bioengineering, University of Washington) was transformed into bacteria first. Briefly, 100 μL *E. coli* BL21(DE3) chemically competent cells were mixed with 4 μL β-ME (ME abbreviation not defined) by gentle swirling and incubated on ice for 10 min. 20 ng pDNA was added into the cell suspension and incubated on ice for 30 min. Cells were heat-shocked for 30 seconds in 42 °C water bath and then placed on ice for 2 min. 0.9 mL preheated (42 °C) S.O.C. (Super Optimal broth with Catabolite repression) Medium was added into cells and incubated at 37 °C with shaking of 225 rpm. 100 μL reaction solution was spread on LB plates containing kanamycin (50 μg/mL) and incubated overnight. Plasmid DNA was recovered from resultant cell cultures using the QIAprep Spin Miniprep Kit (Qiagen).

1.2. Naked pDNA and pDNA/PEI polyplex encapsulation

In vivo-jetPEI polyplexes were formed by mixing pDNA and *in vivo*-jetPEI (Polyplus Transfection®) at a N/P ratio of 7 in equal amount of 5% glucose solution for 15 min at room temperature. To load pDNA/PEI polyplexes into a hydrogel, O-Alg solution was used to re-dissolve the lyophilized polyplexes, and then reacted with S-CS in a syringe as previously described. To prepare naked pDNA loaded hydrogels, 10 μg naked pDNA was directly added into the S-CS solution then mixed with O-Alg solution.

1.3. Polyplex size and distribution

The particle sizes of the pDNA/PEI polyplexes before and after lyophilization were determined by Dynamic Light Scattering (DLS) measurements using a Malvern Zetasizer Nano ZS and the results were reported as the Z-average ± standard deviation. To observe the distribution of pDNA/PEI

polyplexes within the hydrogel, the pDNA was labeled first before polyplex formation by mixing YOYO-1 fluorescent stain (Invitrogen) at a ratio of 0.02 μL of YOYO-1 per μg pDNA for 30 min at room temperature. The pDNA/PEI polyplexes containing either 10 or 20 μg pDNA were loaded into hydrogels and the distribution imaged by fluorescence microscopy.

1.4. In-vitro release test

In order to quantify the release of encapsulated polyplex and naked pDNA from hydrogel, Hoechst dye (H33342, Sigma-Aldrich) was used to determine the concentration of pDNA. Hydrogels were formed using the protocols described above and immersed into 20 mL PBS at 37 °C. PBS solutions were collected and replaced with fresh PBS of the same volume every day. To measure the amount of polyplex released from hydrogel, 90 μL heparin (1 mg/mL) were mixed with 90 μL released samples for 15 min to extract pDNA from polyplex. 180 μL Hoechst dye (0.4 μg/mL in TNE buffer (0.2 M NaCl, 10 mM Tris, 1.3 mM EDTA)) was added and mixed gently by pipetting for 10 min. The fluorescent intensity was measured at an excitation wavelength = 350 nm by plate reader. The readout was converted into mass DNA using a standard curve measured based on naked pDNA. To measure the naked DNA released from hydrogel, 180 μL released samples were mixed with Hoechst dye of the same volume directly. Plasmid DNA was quantified by plate reader as well after 10 min. The presence of heparin/PEI was not found to affect the binding efficiency of the Hoechst dye to DNA nor did the heparin/PEI interfere with the fluorescence reading.

The total amount of accumulative pDNA released over the time was calculated from Eq. (1):

$$M_{ACC}(t) = \sum_{t=0}^{t} V_S C_{pDNA}(t) \quad (1)$$

where M_{ACC} (t) = total amount of pDNA released upto time t, [M]; V_S = sample volume [L^3]; C_{pDNA} (t) = concentration of pDNA at time = t, [M/L^3].

The cumulative percent pDNA release over time is calculated using Eq. (2):

$$\text{Accumulative \% released} = \sum_{t=0}^{t} \left(\frac{M_{ACC(t)}}{M_{TOTAL}}\right) x\ 100\% \qquad (2)$$

where M_{TOTAL} = the total amount of pDNA loaded into each sample.

The release kinetics was analyzed *via* power function fitting and linear analysis by Origin 8.5 software.

1.5. In-vitro transfection

BHK, DC 2.4 and JAWsII cells were seeded in treated 24-well plate at 150,000 cells/well. Cells were incubated at 37 °C for 24 hours before a transfection assay. *In-vivo* jetPEI polyplexes were prepared as described previously using pMAX-GFP, and added to wells at a concentration of 1.5 μg DNA/well as positive control groups. 50 μL polyplex encapsulated within hydrogel was injected into each well and the medium was replaced by 1 mL fresh medium without penicillin-streptomycin. At each time point, cells were imaged by a Zeiss Axio Observer Z1 fluorescence microscope.

2. Results and discussion

2.1. Polyplex formation and distribution

DNA polyplexes were formed by mixing plasmid DNA with linear PEI at a N/P ratio of 7. The lyophilization process decreased the particle size from 182.3 nm to 165.5 nm. The DNA/PEI polyplexes were encapsulated into chitosan-alginate hydrogels by distributing the lyophilized polyplexes within the gel precursors prior to crosslinking. We hypothesized that the distribution of nanoparticles within hydrogel matrix would be closely related to the release behavior. The distribution of pDNA polyplexes within the hydrogel is influenced by numerous factors such as loading density, hydrogel properties, and mixing conditions. To ensure the polyplexes were evenly distributed throughout the hydrogels, different amounts of fluorescently labeled polyplexes were incorporated inside two hydrogels with various chitosan-alginate composition. It was observed that polyplexes dispersed uniformly in 10CS/50Alg hydrogel for both 10 and 20 μg pDNA loading densities (**Figure 4.1 b, c**). However, polyplex aggregation was observed when encapsulated into 15CS/100Alg hydrogel (**Figure 4.1 e, f**). The main reason for this difference was that the highly concentrated chitosan polymer due to its high viscosity blocked the migration or diffusion of polyplexes during the crosslinking process. As a result, polyplex aggregation occurred even though less polyplexes were loaded.

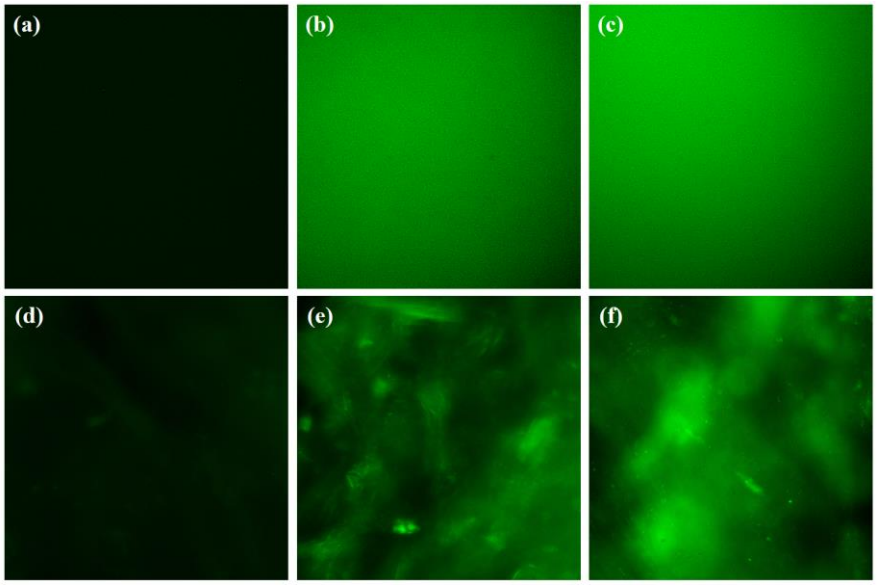

Figure 4.1 DNA/PEI polyplex distribution inside the 10CS/50Alg hydrogel (a-c) and 15CS/100Alg hydrogel (d-f). Pure hydrogels (a, d) and polyplex encapsulated hydrogels containing 10 μg DNA/300 μL gel (b, e) and 20 μg DNA/300 μL gel (c, f) were imaged by an inverted fluorescence microscope (10 ×).

2.2. Release behavior and kinetics

Biodegradable polymeric matrices, especially hydrogels, are widely used in the development of controlled delivery systems. In general, diffusion and material degradation are considered to be the main driving forces for drug release.[47][48] Recently, numerous mathematical models have been developed to describe the release kinetics from biodegradable polymer systems.[49][50]

The *in-vitro* release of naked DNA and DNA polyplexes from hydrogels was quantified by Hoechst dye that stained the released double stranded DNA in PBS.[51] It was found that naked DNA had a burst release in the first 3 days from both hydrogels (**Figure 4.2 a, b**). The burst release was attributed to the degradation of hydrogel in the initial period as well as pDNA leaving from the exterior of the hydrogel, which is suggested by the mass loss in the first few days *in vitro*. Typically, 10 μg DNA was released from 10CS/50Alg and 15CS/100Alg hydrogel with 55.1% and 66.6% in total at 14 days, respectively. In the initial 3 days, 15CS/100Alg hydrogel showed a burst release of 64.2% naked DNA. The release of 20 μg naked DNA had the same tendency with

that of 10 μg DNA, but exhibited a lower release rate. It is possible that the aggregation of DNA molecules at the higher concentration in hydrogel matrix retarded its release.

In contrast, DNA polyplexes were released continuously from the hydrogels (**Figure 4.2 c, d**). 75.9% and 37.2% of DNA polyplexes with 10 μg DNA were released from 10CS/50Alg and 15CS/100Alg hydrogel over 14 days, respectively. Less polyplexes were released sustainably with a lower release rate when more DNA polyplexes were loaded. The shape of the cumulative release curves fit the power function described by the Korsmeyer Model ($\frac{M_t}{M_\infty} = kt^n$) very well regardless of the total amount of polyplex loading or the composition of hydrogel.[52] This correlation suggests that the DNA polyplexes were released from the hydrogel mainly by diffusion. A diffusivity can be calculated from the constant *k*, the slope of $\frac{M_t}{M_\infty}$ vs. $\sqrt{t}$ (**Figure 4.3**), since the diffusivity is proportional to k^2 by simplifying the following well known equation that describes molecular diffusion in polymer matrix.[47]

$$\frac{M_t}{M_\infty} = 1 - \frac{8}{\pi^2}\sum \frac{1}{(2n+1)^2} exp\left\{-\frac{D(2n+1)^2\pi^2 t}{L^2}\right\} \sim 4\sqrt{\frac{D}{L^2\pi}} \cdot \sqrt{t}$$

Here, L is the hydrogel thickness (L=3.67mm). The diffusivity (*D*) could be expressed as follow:

$$D = \pi(\frac{k}{4})^2 L^2$$

The diffusivity of polyplexes with 10 and 20 μg DNA within 10CS/50Alg hydrogel were 1.25×10^{-8} and 4.34×10^{-9} cm^2/sec, respectively. The diffusivity of polyplex in 15CS/100Alg hydrogel decreased to 3.55×10^{-9} and 9.26×10^{-10} cm^2/sec, respectively. One plausible reason is that the stronger crosslinking of 15CS/100Alg hydrogel impedes the diffusion of polyplex. The decreasing of diffusivity by loading more polyplexes is mainly attributed to the aggregation of the nanoparticles.

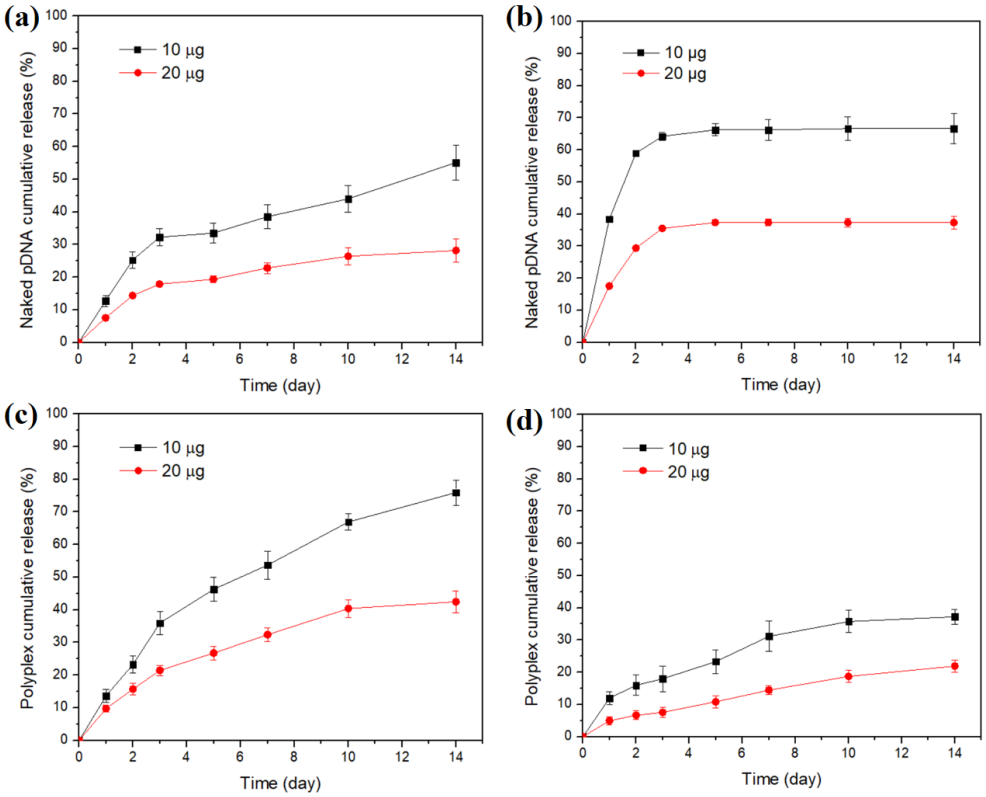

Figure 4.2 Cumulative release of naked DNA and DNA polyplex from 10CS/50Alg hydrogel (a, c) and 15CS/100Alg hydrogel (b, d) at 37 ºC. Values reported are an average n=3, ±standard deviation.

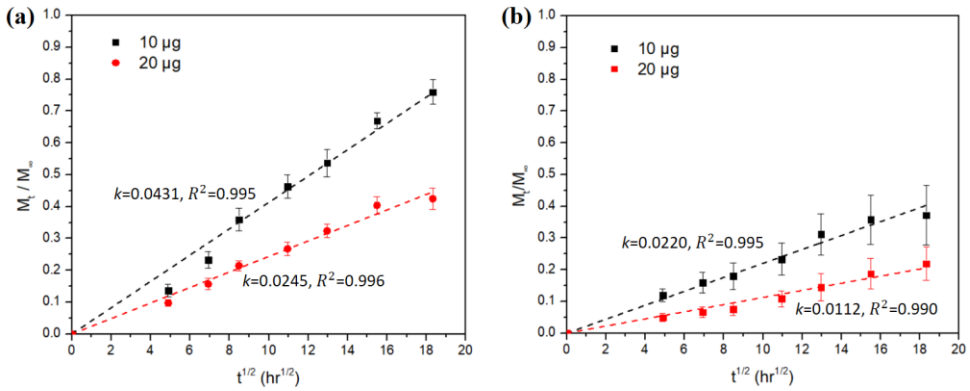

Figure 4.3 Linear fitting by Origin 8.5.1. software to calculate the diffusivity of DNA/PEI polyplex in 10CS/50Alg hydrogel (a) and 15CS/100Alg hydrogel (b).

2.3. In-vitro transfection

Results proved that pMAX-GFP had a higher transfection efficiency when delivered by the linear PEI because both fibroblast and dendritic cells were found transfected as a function of time (**Figure 4.4**). In addition, it was found that fibroblasts were much easier to transfect than dendritic cells, which to be expected because immature dendritic cells engulf pathogens (e.g. bacteria) mainly through macropinocytosis pathways, while fibroblast utilize clathrin-dependent endocytosis for cellular uptake. JAWsII cells were more difficult to transfect than DC 2.4 cells, although both are dendritic cells. Based on the morphology of cells, *in-vivo* jetPEI exhibited a mild toxicity to cells because most of the cells were healthy after culturing for 5 days based on the shape and size of cells compared to the control group.

To test the gene delivery behavior of the hydrogels, lyophilized polyplexes were dissolved in O-Alg solution first and then reacted with S-CS solution to form hydrogel. 50 μL of polyplex loaded hydrogel containing about 1.7 μg DNA was injected into each well. The same amount of naked DNA was also encapsulated into hydrogels, but no transfection was observed in either cell lines in 5 days. **Figure 4.5** shows BHK, DC 2.4 and JAWsII cells transfection by polyplex encapsulated hydrogel after 1-day, 3-day and 5-day culture. More BHK cells were observed to be transfected at 5 days, which is demonstrated by clear GFP signals. In addition, gene expression of dendritic cells was observed at 5 days although some weak GFP expression was observed at 3 days as well. The lower transfection efficiency of polyplexes delivered *via* hydrogel ascribed to a slow and continuous release. In addition, the chitosan or alginate might also influence the polyplex structure because they were both charged.[53] As a result, the particle size of some polyplexes released from hydrogel may have increased to the point that they would be too large to be taken up by cells.

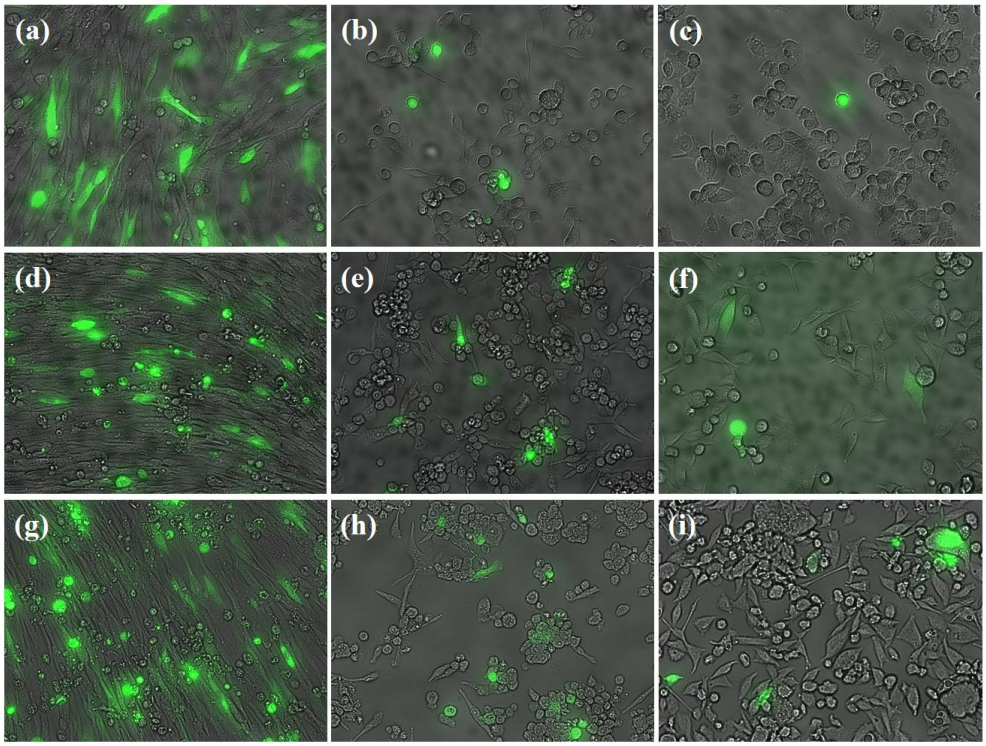

Figure 4.4 *In-vitro* pDNA/PEI polyplex transfection of BHK (left), DC 2.4 (middle) and JAWsII cells (right) after 1 day (a, b, c), 3 days (d, e, f) and 5 days (g, h, i).

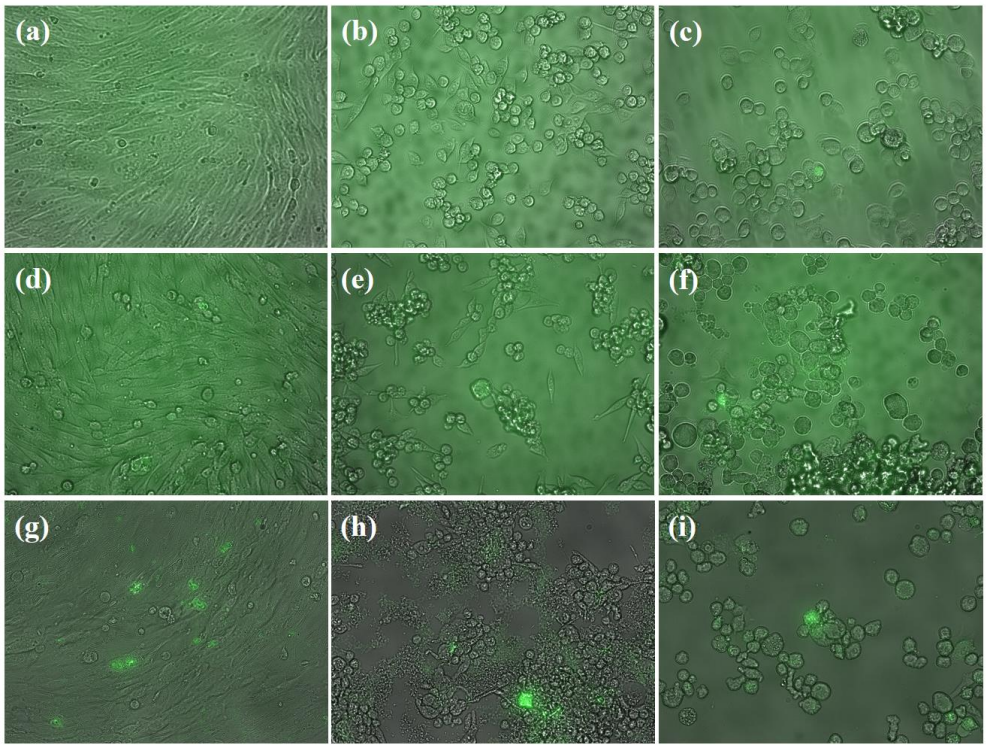

Figure 4.5 BHK (left), DC 2.4 (middle) and JAWsII (right) transfection by polyplex encapsulated hydrogel after 1 day (a, b, c), 3 days (d, e, f) and 5 days (g, h, i).

3. Conclusions

Nanoparticle "polyplexes" were formed by mixing pDNA (pMAX-GFP) with linear PEI in a N/P=7. The lyophilized polyplexes with a size of 165.5 nm were encapsulated into chitosan:alginate injectable hydrogels. Polyplex *in-vitro* release kinetics from various hydrogels were quantified. Results show that between 40-75% of pDNA/PEI polyplexes were continuously released from 10CS/50Alg hydrogel over 14 days mainly by diffusion, not hydrogel degradation. In addition, the diffusivity of polyplex within hydrogel was calculated and the value varied with polyplex loading and hydrogel composition. In general, the 15CS/100Alg hydrogel with a stronger crosslinking inhibited the diffusion of polyplex. The *in-vitro* transfection of fibroblast (BHK) and dendritic cells (DC 2.4 and JAWsII cells) was then quantified by observing GFP gene expression at 1 day, 3 days and 5 days. Both fibroblasts and dendritic cells exhibited GFP gene transfection and high cell viability. Fibroblasts were found much easier to transfect than dendritic cells *in vitro*. When polyplexes were encapsulated within hydrogels, the released polyplexes showed no transfection of either BHK cells or DCs in the first 3 days. But GFP expression was observed at Day 5 with BHK expression higher than either dendritic cell lines. This suggests that the chitosan-alginate hydrogel could be a candidate for gene delivery, but more optimization is necessary to improve the transfection efficiency.

Chapter 5 Overall conclusions

1. Summary of thesis

In my master thesis, an injectable chitosan/alginate hydrogel was well developed, and the properties were systematically characterized. The hydrogel could be injected through syringe after mixing N-succinyl chitosan and oxidized alginate solution for about 2 minutes. The *in-situ* forming homogeneous hydrogel has elastic properties with a small deformation, and the compression modulus was similar to that of soft tissues. The high swelling ratio but low protein adsorption proved its hydrophilic properties. Most importantly, the hydrogel is degradable, and protein had a function of accelerating its degradation process. These hydrogels exhibited low cell toxicity as proven by a cell viability test using both fibroblast and dendritic cell lines.

To serve as a gene delivery system, the hydrogel was used to encapsulate pDNA/PEI polyplexes. The *in-vitro* release test suggested that the polyplexes were released continuously for at least 2 weeks by diffusion. Both fibroblasts and dendritic cells exhibited GFP gene expression at 5 days by polyplexes encapsulated hydrogel. In general, the chitosan/alginate hydrogel system showed an exciting potential of application on gene delivery.

2. Future Work

There are plenty of merits of the chitosan/alginate hydrogel which were demonstrated by the characterizations and the *in-vitro* tests of this study. Nevertheless, the key issue is the low transfection efficiency when the polyplexes are delivered by hydrogel. New transfection reagents will be used to improve the cellular uptake and transfection. Specifically, lipid-based structures have been widely reported as great candidates for nucleic acid delivery and could replace the PEI used here.

Next, an *in-vivo* gene delivery study is necessary to quantify pDNA polyplexes or lipoplexes DNA release, polyplex tracking, and gene expression detecting under clinical conditions.

Reference

[1] M. Ramamoorth and A. Narvekar, "Non viral vectors in gene therapy - An overview," *J. Clin. Diagnostic Res.*, vol. 9, no. 1, p. GE01-GE06, 2015.

[2] M. S. Al-Dosari and X. Gao, "Nonviral Gene Delivery: Principle, Limitations, and Recent Progress," *AAPS J.*, vol. 11, no. 4, pp. 671–681, 2009.

[3] H. Yin, R. L. Kanasty, A. A. Eltoukhy, A. J. Vegas, J. R. Dorkin, and D. G. Anderson, "Non-viral vectors for gene-based therapy," *Nat. Rev. Genet.*, vol. 15, no. 8, pp. 541–555, 2014.

[4] C. X. He, Y. Tabata, and J. Q. Gao, "Non-viral gene delivery carrier and its three-dimensional transfection system," *Int. J. Pharm.*, vol. 386, no. 1–2, pp. 232–242, 2010.

[5] J. P. Lim and P. A. Gleeson, "Macropinocytosis: An endocytic pathway for internalising large gulps," *Immunol. Cell Biol.*, vol. 89, no. 8, pp. 836–843, 2011.

[6] A. Aied, U. Greiser, A. Pandit, and W. Wang, "Polymer gene delivery: Overcoming the obstacles," *Drug Discov. Today*, vol. 18, no. 21–22, pp. 1090–1098, 2013.

[7] D. G. Anderson, D. M. Lynn, and R. Langer, "Zuschriften," pp. 3261–3266, 2003.

[8] M. Keeney, S. Onyiah, Z. Zhang, X. Tong, L. H. Han, and F. Yang, "Modulating polymer chemistry to enhance non-viral gene delivery inside hydrogels with tunable matrix stiffness," *Biomaterials*, vol. 34, no. 37, pp. 9657–9665, 2013.

[9] G. Feng *et al.*, "Injectable nanofibrous spongy microspheres for NR4A1 plasmid DNA transfection to reverse fibrotic degeneration and support disc regeneration," *Biomaterials*, vol. 131, pp. 86–97, 2017.

[10] Y. Yang *et al.*, "A novel gene delivery composite system based on biodegradable folate-poly (ester amine) polymer and thermosensitive hydrogel for sustained gene release," *Sci. Rep.*, vol. 6, no. October 2015, p. 21402, 2016.

[11] Y. Lei and T. Segura, "DNA delivery from matrix metalloproteinase degradable poly(ethylene glycol) hydrogels to mouse cloned mesenchymal stem cells," *Biomaterials*, vol. 30, no. 2, pp. 254–265, 2009.

[12] M. W. Konstan *et al.*, "Compacted DNA Nanoparticles Administered to the Nasal Mucosa of Cystic Fibrosis Subjects Are Safe and Demonstrate Partial to Complete Cystic Fibrosis Transmembrane Regulator Reconstitution," *Hum. Gene Ther.*, vol. 15, no. 12, pp. 1255–1269, 2004.

[13] H. Song *et al.*, "Cationic lipid-coated PEI/DNA polyplexes with improved efficiency and reduced cytotoxicity for gene delivery into mesenchymal stem cells," *Int. J. Nanomedicine*, vol. 7, pp. 4637–4648, 2012.

[14] S. Şenel and S. J. McClure, "Potential applications of chitosan in veterinary medicine," *Adv. Drug Deliv. Rev.*, vol. 56, no. 10, pp. 1467–1480, 2004.

[15] A. A. Foster, C. T. Greco, M. D. Green, T. H. Epps, and M. O. Sullivan, "Light-mediated

activation of siRNA release in diblock copolymer assemblies for controlled gene silencing," *Adv. Healthc. Mater.*, vol. 4, no. 5, pp. 760–770, 2015.

[16] W.-F. Lai, "Cyclodextrins in non-viral gene delivery," *Biomaterials*, vol. 35, no. 1, pp. 401–411, 2014.

[17] Y. Gao *et al.*, "Highly Branched Poly(β-amino esters) for Non-Viral Gene Delivery: High Transfection Efficiency and Low Toxicity Achieved by Increasing Molecular Weight," *Biomacromolecules*, vol. 17, no. 11, pp. 3640–3647, 2016.

[18] M. E. Favretto, A. Krieg, S. Schubert, U. S. Schubert, and R. Brock, "Multifunctional poly(methacrylate) polyplex libraries: A platform for gene delivery inspired by nature," *J. Control. Release*, vol. 209, pp. 1–11, 2015.

[19] H. Zhang and S. V. Vinogradov, "Short biodegradable polyamines for gene delivery and transfection of brain capillary endothelial cells," *J. Control. Release*, vol. 143, no. 3, pp. 359–366, 2010.

[20] C. Dufès, I. F. Uchegbu, and A. G. Schätzlein, "Dendrimers in gene delivery," *Adv. Drug Deliv. Rev.*, vol. 57, no. 15, pp. 2177–2202, 2005.

[21] C. Madeira *et al.*, "Nonviral Gene Delivery to Mesenchymal Stem Cells Using Cationic Liposomes for Gene and Cell Therapy," *J. Biomed. Biotechnol.*, vol. 2010, pp. 1–12, 2010.

[22] D. Martinez *et al.*, "Extracellular Acidosis Triggers the Maturation of Human Dendritic Cells and the Production of IL-12," *J. Immunol.*, vol. 179, no. 3, pp. 1950–1959, 2007.

[23] Y. Inoh, M. Nagai, K. Matsushita, M. Nakanishi, and T. Furuno, "Gene transfection efficiency into dendritic cells is influenced by the size of cationic liposomes/DNA complexes," *Eur. J. Pharm. Sci.*, vol. 102, pp. 230–236, 2017.

[24] J. Kim *et al.*, "Injectable, spontaneously assembling, inorganic scaffolds modulate immune cells in vivo and increase vaccine efficacy," *Nat. Biotechnol.*, vol. 33, no. 1, pp. 61–69, 2014.

[25] K. Y. Lee and D. J. Mooney, "Hydrogels for Tissue Engineering Applications," *Chem. Rev.*, vol. 101, no. 7, pp. 1869–1879, 2001.

[26] M. Yoshida *et al.*, "Complexation hydrogels as potential carriers in oral vaccine delivery systems," *Eur. J. Pharm. Biopharm.*, vol. 112, pp. 138–142, 2017.

[27] S. Lü, M. Liu, and B. Ni, "An injectable oxidized carboxymethylcellulose/N-succinyl-chitosan hydrogel system for protein delivery," *Chem. Eng. J.*, vol. 160, no. 2, pp. 779–787, 2010.

[28] Y. Lei, M. Rahim, Q. Ng, and T. Segura, "Hyaluronic acid and fibrin hydrogels with concentrated DNA/PEI polyplexes for local gene delivery," *J. Control. Release*, vol. 153, no. 3, pp. 255–261, 2011.

[29] Z. Li *et al.*, "Controlled gene delivery system based on thermosensitive biodegradable hydrogel," *Pharm. Res.*, vol. 20, no. 6, pp. 884–888, 2003.

[30] J. Zhang, A. Sen, E. Cho, J. S. Lee, and K. Webb, “Poloxamine/fibrin hybrid hydrogels for non-viral gene delivery,” *J. Tissue Eng. Regen. Med.*, vol. 11, no. 1, pp. 246–255, 2017.

[31] A. Sivashanmugam, R. Arun Kumar, M. Vishnu Priya, S. V. Nair, and R. Jayakumar, “An overview of injectable polymeric hydrogels for tissue engineering,” *Eur. Polym. J.*, vol. 72, pp. 543–565, 2015.

[32] E. R. West, M. Xu, T. K. Woodruff, and L. D. Shea, “Physical properties of alginate hydrogels and their effects on in vitro follicle development,” *Biomaterials*, vol. 28, no. 30, pp. 4439–4448, 2007.

[33] V. Guarino, T. Caputo, R. Altobelli, and L. Ambrosio, “Degradation properties and metabolic activity of alginate and chitosan polyelectrolytes for drug delivery and tissue engineering applications,” *AIMS Mater. Sci.*, vol. 2, no. 4, pp. 497–502, 2015.

[34] S. N. S. Anumolu *et al.*, “Doxycycline hydrogels with reversible disulfide crosslinks for dermal wound healing of mustard injuries,” *Biomaterials*, vol. 32, no. 4, pp. 1204–1217, 2011.

[35] G. Peng *et al.*, “In situ formation of biodegradable dextran-based hydrogel via Michael addition,” *J. Appl. Polym. Sci.*, vol. 127, no. 1, pp. 577–584, 2013.

[36] S. J. Buwalda, P. J. Dijkstra, and J. Feijen, “Biodegradable, in situ forming poly(ethylene glycol)-poly(lactide) hydrogels by Michael addition chemistry,” *J. Control. Release*, vol. 152, Suppl, no. 0, pp. e199–e201, 2011.

[37] K. M. Park, Y. Lee, J. Y. Son, D. H. Oh, J. S. Lee, and K. D. Park, “Synthesis and characterizations of in situ cross-linkable gelatin and 4-arm-PPO-PEO hybrid hydrogels via enzymatic reaction for tissue regenerative medicine,” *Biomacromolecules*, vol. 13, no. 3, pp. 604–611, 2012.

[38] S. G. J. Postma, I. N. Vialshin, C. Y. Gerritsen, M. Bao, and W. T. S. Huck, “Preprogramming Complex Hydrogel Responses using Enzymatic Reaction Networks,” *Angew. Chemie Int. Ed.*, vol. 56, no. 7, pp. 1794–1798, 2017.

[39] H. Chen *et al.*, “Covalently antibacterial alginate-chitosan hydrogel dressing integrated gelatin microspheres containing tetracycline hydrochloride for wound healing,” *Mater. Sci. Eng. C*, vol. 70, no. Part 2, pp. 287–295, 2017.

[40] M. Fan *et al.*, “Covalent and injectable chitosan-chondroitin sulfate hydrogels embedded with chitosan microspheres for drug delivery and tissue engineering,” *Mater. Sci. Eng. C*, vol. 71, pp. 67–74, 2017.

[41] T. Boontheekul, H. J. Kong, and D. J. Mooney, “Controlling alginate gel degradation utilizing partial oxidation and bimodal molecular weight distribution,” *Biomaterials*, vol. 26, no. 15, pp. 2455–2465, 2005.

[42] S. L. Levengood and M. Zhang, “Chitosan-based scaffolds for bone tissue engineering,” *J Mater Chem B Mater Biol Med*, vol. 2, no. 21, pp. 3161–3184, 2014.

[43] I. Aranaz *et al.*, “Functional Characterization of Chitin and Chitosan,” *Curr. Chem. Biol.*,

vol. 3, pp. 203–230, 2009.

[44] U. Rottensteiner *et al.*, “In vitro and in vivo biocompatibility of alginate dialdehyde/gelatin hydrogels with and without nanoscaled bioactive glass for bone tissue engineering applications,” *Materials (Basel).*, vol. 7, no. 3, pp. 1957–1974, 2014.

[45] W. S. Kim, D. J. Mooney, P. R. Arany, K. Lee, N. Huebsch, and J. Kim, “Adipose Tissue Engineering Using Injectable, Oxidized Alginate Hydrogels,” *Tissue Eng. Part A*, vol. 18, no. 7–8, pp. 737–743, 2011.

[46] K. H. Bouhadir, K. Y. Lee, E. Alsberg, K. L. Damm, K. W. Anderson, and D. J. Mooney, “Degradation of partially oxidized alginate and its potential application for tissue engineering,” *Biotechnol. Prog.*, vol. 17, no. 5, pp. 945–950, 2001.

[47] S. Dash, P. N. Murthy, L. Nath, and P. Chowdhury, “Kinetic modeling on drug release from controlled drug delivery systems.,” *Acta Pol. Pharm.*, vol. 67, no. 3, pp. 217–23, 2010.

[48] F. Yao and J. K. Weiyuan, “Drug Release Kinetics and Transport Mechanisms of Non-degradable and Degradable Polymeric Delivery Systems,” *Expert Opin. Drug Deliv.*, vol. 7, no. 4, pp. 429–444, 2010.

[49] I. Katzhendler, A. Hoffman, A. Goldberger, and M. Friedman, “Modeling of drug release from erodible tablets.,” *J. Pharm. Sci.*, vol. 86, no. 1, pp. 110–115, 1997.

[50] J. Siepmann and N. A. Peppas, “Higuchi equation: Derivation, applications, use and misuse,” *Int. J. Pharm.*, vol. 418, no. 1, pp. 6–12, 2011.

[51] P. G. Penketh, K. Shyam, and a C. Sartorelli, “Fluorometric assay for the determination of DNA-DNA cross-links utilizing Hoechst 33258 at neutral pH values.,” *Anal. Biochem.*, vol. 252, no. 1, pp. 210–3, 1997.

[52] R. W. Korsmeyer, R. Gurny, E. Doelker, P. Buri, and N. A. Peppas, “Mechanisms of solute release from porous hydrophilic polymers,” *Int. J. Pharm.*, vol. 15, no. 1, pp. 25–35, 1983.

[53] A. N. Wilson, M. Blenner, and A. Guiseppi-Elie, “Polyplex formation influences release mechanism of mono- and di-valent ions from phosphorylcholine group bearing hydrogels,” *Polymers (Basel).*, vol. 6, no. 9, pp. 2451–2472, 2014.